Table 3. Tabulated values of variables and correlating constants

Variables or constants	Test run no. 1	2	3	4	5	6	7	8	9	10	Average	Error
C_1	2.72	2.72	2.63	2.18	2.17	2.23	2.08	2.14	1.90	1.90	2.27	±20%
C_2	−200.6	−189.2	−179.8	−233.2	−233.8	−222.0	−257.0	−249.2	−272.2	−273.0	−231.0	±20%
g_1	8.9	8.6	9.9	8.3	8.2	7.8	6.9	8.3	6.8	6.9	8.1	±22%
g_2	−191.0	−190.9	−193.3	−218.5	−218.9	−256.3	−286.3	−292.7	−253.1	−252.6	−253.4	±17%
$\dot{m}_t$	8.6	8.4	9.8	9.1	8.5	8.1	7.3	8.1	7.1	7.3	8.2	±13%
$\bar{h}_{fg}$	2217.9	2196.3	1989.9	1876.4	1936.2	2074.5	2167.3	1985.7	1983.1	1792.4	2021.4	±11%

that the present correlation for both heat transfer and mass flow rates is consistent with each other as far as the correlating constants illustrating the thermal characteristics of the present heat-pipe heat exchangers are concerned. The other is that the heat transfer rate seems uniquely determined once $\dot{m}_t$ and c_1 are found. It appears that the methodology under investigation does not generate any more limitations on the heat transfer rate of a heat-pipe heat exchanger.

The total mass flux as well as the average latent heat are also tabulated in Table 3 for ten cases with the maximum error about ±20%. The error in the variable and the correlating constant was defined as the percentage deviation between the average value for total test runs and the value of each individual case. It is, therefore, concluded that the desired correlation for the heat transfer rate of a heat-pipe heat exchanger under the present configuration can be expressed in the form of

$$\frac{Q}{Q_0} = c_1(1-e^{c_2\varepsilon_v})$$

where $c_1 = 2.27 \pm 20\%$, $c_2 = -231.0 \pm 20\%$. It seems that c_1 and c_2 are independent of the specifications of the individual heat pipe. Further studies may include the experimental verification of the present results.

CONCLUSIONS

A simplified but relatively generalized method is developed and used to predict the thermal performance of the heat-pipe heat exchanger for any staggered type alignment. The model has been tested based on the results from previous investigators. The resultant thermal performance is correlated in the form

$$\frac{Q}{Q_0} = 2.27(1-e^{-2.31\varepsilon_v})$$

which may provide thermal design data for a heat-pipe heat exchanger configuration applicable to waste heat recovery systems.

Acknowledgements—The author would like to express his appreciation to Mr S. S. Liou for performing the numerical calculations for this study. Special thanks go to Mr C. T. Liauh for typing the manuscript.

REFERENCES

1. S. W. Chi, *Heat Pipe Theory and Practice*, Chap. 1. McGraw-Hill, New York (1976).
2. J. O. Amode and K. T. Feldman, Preliminary analysis of heat pipe heat exchangers for heat recovery, ASME Paper No. 75-WA/HT-36 (1976).
3. Y. Lee and A. Bedrossian, The characteristics of heat exchangers using heat pipes or thermosyphons, *Int. J. Heat Mass Transfer* **21**, 221–229 (1978).
4. B. J. Huang and J. T. Tsuei, A method of analysis for heat pipe heat exchangers, *Int. J. Heat Mass Transfer* **28**, 553–562 (1985).

Int. J. Heat Mass Transfer. Vol. 30, No. 8, pp. 1762–1765, 1987
Printed in Great Britain

0017-9310/87 $3.00 + 0.00
Pergamon Journals Ltd.

Radiative cooling of a solidifying droplet layer including absorption and scattering

ROBERT SIEGEL
NASA–Lewis Research Center, MS 5–9, Office of the Chief Scientist, 21000 Brookpark Road, Cleveland, OH 44135, U.S.A.

(*Received* 1 *December* 1986 *and in final form* 17 *February* 1987)

INTRODUCTION

A POWER generating device for space applications requires a radiator for waste heat dissipation. As the power requirements increase (e.g. for a space station), a conventional radiator, such as a tube and fin design, could become so large and heavy that it would be impractical to launch and erect in space. A radiator has been proposed in the literature that may be much lighter and easier to deploy; it would utilize streams of hot liquid drops passing directly through space so that energy would be lost by transient radiative cooling [1]. Recent research and analysis on this type of radiator are given in refs. [2–4]. To better utilize the energy transport ability of the drops, it may be useful to have the drops solidify, thereby taking advantage of their latent heat of fusion. This could also reduce evaporation losses from the drops. The liquid drop radiator would consist of thousands of individual directed streams that form a layer of drops (Fig. 1). If the initial temperature of this array of drops is near their freezing point, the subsequent radiative cooling will initiate solidification. During the phase change that follows, the two-phase layer will remain at uniform tempera-

NOMENCLATURE

a	absorption coefficient of drop-filled layer
D	thickness of drop-filled layer
E_1, E_2	exponential integral functions, $E_n(x) = \int_0^1 \mu^{n-2} \exp(-x/\mu)\,d\mu$
I	source function in absorbing–scattering layer; $\tilde{I} = \pi I/\sigma T_f^4$
q_r	radiative heat flow per unit area and time
T_e	temperature of surrounding environment, $T_e = 0$
T_f	solidification temperature
u	velocity distribution across drop-filled layer
$\bar{u}$	integrated mean value of u
$\tilde{V}$	local liquid fraction of drops in layer, V_l/V_d
V_d	volume of drops per unit volume of layer
V_l	volume of liquid per unit volume of layer
x	coordinate across width of layer
Z	dimensionless coordinate, $(\sigma T_f^4/\rho\lambda\bar{u})(z/D)$
z	coordinate along length of layer in flow direction
z_0	location where $\tilde{V}$ first reaches zero; $Z_0 = Z(z_0)$.

Greek symbols

ε	emittance of layer
κ	optical coordinate, $(a+\sigma_s)x$; κ_D optical thickness, $(a+\sigma_s)D$
κ^*	dummy variable of integration
λ	latent heat per unit mass of layer containing drops
ρ	density of layer containing drops
σ_s	scattering coefficient of drop-filled layer
Ω	albedo for scattering, $\sigma_s/(a+\sigma_s)$.

ture. This will maintain a higher layer emittance than for a layer where the outer portion has become cool as a result of sensible heat loss.

In this technical note, a rather simple solution will be obtained for the transient cooling of a solidifying layer filled with drops that can emit and scatter radiation. The velocity distribution across the layer can be nonuniform, as shown in Fig. 1. Although the layer remains at uniform temperature during solidification, the outer portions lose heat most rapidly. This produces a variation along the length of the layer in the distribution of liquid concentration across the layer. The analytical solution applies until any local region within the layer becomes completely solidified. The results provide the amount of energy that can be dissipated by the two-phase system while it remains at uniform temperature. Another aspect of the solution considers the particular velocity distribution that will maintain a uniform liquid fraction across the entire layer at all locations along the layer length. With this velocity distribution, all of the latent energy in the layer can be radiated away while the layer remains at uniform temperature with a constant emittance.

The radiative cooling of the two-phase layer provides an interesting type of freezing situation, since it does not involve a moving boundary dividing solid and liquid regions. Energy is being dissipated by radiation from throughout the entire partially solidified layer; hence solidification occurs simultaneously throughout the entire layer.

ANALYSIS

The drops in the region in Fig. 1 originate as liquid just slightly above the melting point. As long as the layer does not contain any local region that has become completely solidified it will remain at T_f, and the loss of latent energy by radiative cooling is governed by the energy equation

$$\frac{\rho\lambda u(x)}{V_d}\frac{\partial V_l}{\partial z} = -\frac{\partial q_r}{\partial x}. \tag{1}$$

The derivative in radiative flux for a gray medium with isotropic scattering is given in terms of the source function, I, by [5]

$$-\frac{1}{a+\sigma_s}\frac{\partial q_r}{\partial x} = -\frac{\partial q_r}{\partial \kappa} = 2\pi\int_0^{\kappa_D} I(\kappa^*, z) \times E_1(|\kappa-\kappa^*|)\,d\kappa^* - 4\pi I(\kappa, z). \tag{2}$$

For emission and scattering in a layer at uniform temperature T_f, the source function is [5]

$$I(\kappa) = (1-\Omega)\frac{\sigma T_f^4}{\pi} + \frac{\Omega}{2}\int_0^{\kappa_D} I(\kappa^*)E_1(|\kappa-\kappa^*|)\,d\kappa^*. \tag{3}$$

Note that, since T_f is constant, $I(\kappa)$ is independent of z. By eliminating the integral between equations (2) and (3), the radiative flux derivative is found as

$$-\frac{\partial q_r}{\partial \kappa} = 4\frac{1-\Omega}{\Omega}[\pi I(\kappa) - \sigma T_f^4]. \tag{4}$$

Then the energy equation, equation (1), becomes

$$\rho\lambda\frac{\partial(V_l/V_d)}{\partial z} = 4(a+\sigma_s)\frac{1-\Omega}{\Omega}\frac{\pi I(\kappa)-\sigma T_f^4}{u(\kappa)}. \tag{5}$$

Since $I(\kappa)$ and $u(\kappa)$ are independent of z, equation (5) can be integrated subject to the condition $V_l/V_d = 1$ at $z = 0$ to obtain the solution for V_l/V_d in dimensionless form

$$\tilde{V}(\kappa, Z) = 1 - 4\kappa_D\frac{1-\Omega}{\Omega}\frac{1-\tilde{I}(\kappa)}{u(\kappa)/\bar{u}}Z. \tag{6}$$

Relations when velocity is uniform across layer

In this instance equation (6) simplifies since $u(\kappa)/\bar{u} = 1$. Then at the outer boundary of the layer, $\kappa = 0$, the liquid fraction is

$$\tilde{V}(0, Z) = 1 - 4\kappa_D\frac{1-\Omega}{\Omega}[1-\tilde{I}(0)]Z. \tag{7}$$

Let Z_0 be the axial location where solidification first becomes complete at any local position within the layer. For a uniform velocity this would be at the outer boundary of the layer.

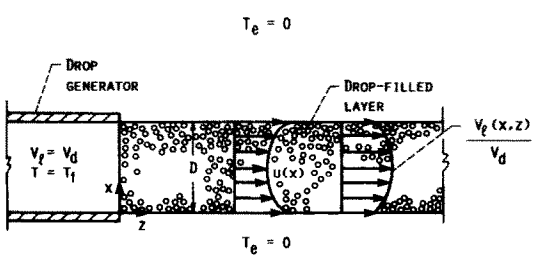

FIG. 1. Geometry of radiating–scattering layer filled with hot solidifying drops and having a non-uniform velocity.

Then $\tilde{V}(0, Z_0) = 0$ and equation (7) yields

$$Z_0 = \frac{1}{4\kappa_D}\frac{\Omega}{1-\Omega}\frac{1}{1-\tilde{I}(0)}, \quad 0 < \Omega < 1. \tag{8a}$$

From equation (3)

$$\frac{1-\tilde{I}(0)}{\Omega} = 1 - \frac{1}{2}\int_0^{\kappa_D} \tilde{I}(\kappa^*)E_1(\kappa^*)\,d\kappa^*$$

so that equation (8a) can be written as

$$Z_0 = \frac{1}{4\kappa_D(1-\Omega)}\frac{1}{1-\frac{1}{2}\int_0^{\kappa_D}\tilde{I}(\kappa^*)E_1(\kappa^*)\,d\kappa^*}.$$

When scattering is absent, $\Omega = 0$ and $\tilde{I} = 1$, so that Z_0 becomes

$$Z_0 = \frac{1}{2\kappa_D}\frac{1}{1+E_2(\kappa_D)}, \quad \Omega = 0. \tag{8b}$$

In the region $0 \leqslant Z \leqslant Z_0$, the entire layer thickness is two-phase and is at temperature T_f. The emittance of a constant temperature layer depends only on its optical thickness and scattering albedo; hence the emittance remains constant between $Z = 0$ and Z_0. Then the fraction of the original latent energy that is emitted in the constant temperature region from $Z = 0$ to Z_0 is

$$\frac{2\varepsilon\sigma T_f^4 z_0}{D\bar{u}\rho\lambda} = 2\varepsilon(\kappa_D, \Omega)Z_0. \tag{9}$$

The $\varepsilon(\kappa_D, \Omega)$ values are given in Table 1 obtained from ref. [4]. The $\tilde{I}(0)$ values needed for evaluation of Z_0 in equation (8a) were obtained from a numerical solution of the integral equation, equation (3). The numerical solution is described in ref. [4] and will not be repeated here.

Relations for non-uniform velocity to yield uniform V_1

If the liquid fraction $\tilde{V}(\kappa, z)$ can be kept uniform across the layer, the entire cross-section will become solid at $z = z_0$. Thus the entire layer will remain two-phase and at uniform temperature while all of the latent energy is lost. To have $\tilde{V}$ be independent of κ, equation (6) shows that $u(\kappa)$ must be proportional to $1-\tilde{I}(\kappa)$. Then

$$\frac{u(\kappa)}{\bar{u}} = \frac{1-\tilde{I}(\kappa)}{\frac{1}{\kappa_D}\int_0^{\kappa_D}[1-\tilde{I}(\kappa)]\,d\kappa}, \quad 0 < \Omega < 1. \tag{10a}$$

Another form for equation (10a) is obtained by substituting $1-\tilde{I}(\kappa)$ from equation (3) to yield

$$\frac{u(\kappa)}{\bar{u}} = \kappa_D \frac{2 - \int_0^{\kappa_D}\tilde{I}(\kappa^*)E_1(|\kappa-\kappa^*|)\,d\kappa^*}{\int_0^{\kappa_D}\left[2 - \int_0^{\kappa_D}\tilde{I}(\kappa^*)E_1(|\kappa-\kappa^*|)\,d\kappa^*\right]d\kappa}.$$

Table 1. Emittance values for drop-filled layer at uniform temperature, $\varepsilon(\kappa_D, \Omega)$

Optical thickness, κ_D	Scattering albedo, Ω					
	0	0.3	0.6	0.8	0.9	0.95
0.2	0.296	0.225	0.140	0.0748	0.0386	0.0197
0.5	0.557	0.449	0.303	0.172	0.0926	0.0481
1.0	0.781	0.667	0.490	0.304	0.173	0.0926
2	0.940	0.846	0.681	0.475	0.297	0.170
3	0.982	0.900	0.757	0.566	0.382	0.233
4	0.994	0.918	0.786	0.612	0.436	0.281
5	0.998	0.924	0.798	0.637	0.470	0.317
10	1.000	0.933	0.808	0.659	0.518	0.389

For the case of no scattering, $\tilde{I} = 1$, and this form is integrated to give

$$\frac{u(\kappa)}{\bar{u}} = \kappa_D \frac{E_2(\kappa) + E_2(\kappa_D - \kappa)}{1 - 2E_3(\kappa_D)}, \quad \Omega = 0. \tag{10b}$$

By substituting equation (10a) into equation (6), the variation of liquid fraction with length becomes

$$\tilde{V}(Z) = 1 - 4\frac{1-\Omega}{\Omega}\left\{\int_0^{\kappa_D}[1-\tilde{I}(\kappa)]\,d\kappa\right\}Z. \tag{11}$$

This is simplified by noting that from equation (4) the integral of $\partial q_r/\partial\kappa$ from $\kappa = 0$ to κ_D yields

$$q_r(\kappa_D) - q_r(0) = 4\frac{1-\Omega}{\Omega}\sigma T_f^4\int_0^{\kappa_D}[1-\tilde{I}(\kappa)]\,d\kappa. \tag{12}$$

From symmetry $q_r(\kappa_D) = -q_r(0) = \varepsilon\sigma T_f^4$. Then by use of equation (12), equation (11) gives the variation of $\tilde{V}$ with length as

$$\tilde{V}(Z) = 1 - 2\varepsilon Z. \tag{13}$$

Complete solidification, $\tilde{V}(Z) = 0$, is reached when

$$Z_0 = \frac{1}{2\varepsilon}. \tag{14}$$

The values of $\varepsilon(\kappa_D, \Omega)$ are given in Table 1.

RESULTS AND DISCUSSION

The drop-filled layer starts in all liquid form, and for a layer with uniform velocity it remains two-phase across its entire width up to axial location z_0, as given in dimensionless form by equations (8a) and (8b). The layer emittance remains high at the value for a constant temperature layer. The values of $\tilde{I}(0)$ for equation (8a) were obtained for various κ_D and Ω from the numerical solution of equation (3), and the resulting z_0 for a uniform velocity layer are given in Fig. 2. The ordinate is the quantity $Z_0\kappa_D$ calculated from equation (8), and the curves presented in this way are rather insensitive to the optical thickness so that values can be readily interpolated for other κ_D values. The z_0 increases substantially as Ω is increased. This is the result of a decreased layer emittance, and also the fact that increased scattering makes the energy loss more uniform from within the layer. This allows

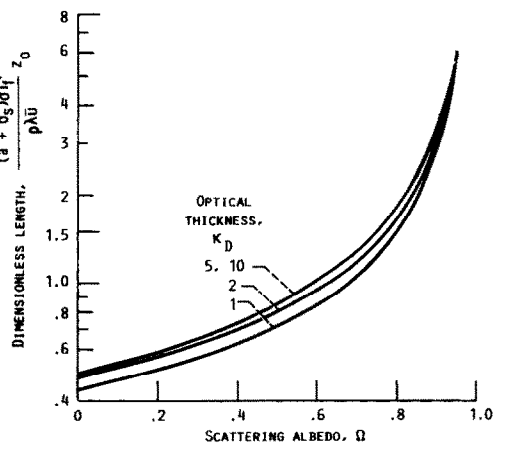

FIG. 2. Length of completely two-phase region for layer having a uniform velocity.

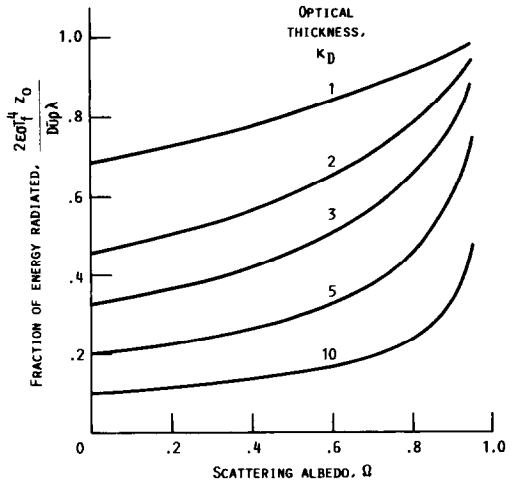

FIG. 3. Fraction of latent energy radiated away while layer with uniform velocity remains completely two-phase.

more energy to be dissipated before the drops at the outer edges of the layer become completely solid. For $z > z_0$, the outer regions of the layer become completely solidified and then decrease in temperature because of sensible heat loss; this will yield a reduced emittance for the layer.

The other quantity of interest for a layer with uniform velocity is the total amount of energy that can be radiated away while the layer remains at uniform temperature, equation (9). This is given in Fig. 3 as a function of the layer optical thickness and scattering albedo. The largest energy fraction radiated away will occur when the local radiative loss from within the layer is most uniform. This occurs when the layer is optically thin, or when the albedo is large so that scattering produces a more uniform distribution of energy throughout the layer. This delays the onset of complete local solidification in the layer.

For the layer with non-uniform velocity, the Z_0 is given by the simple relation equation (14). The velocity distribution required to achieve this is in equations (10a) and (10b). Equation (10a) was evaluated using the numerical solution in ref. [4] for the integral equation, equation (3), and the velocity distributions for $\kappa_D = 2$ and 5 are in Fig. 4 for various values of Ω. For an optically thick region (large κ_D), the outer portions of the drop-filled layer cool more readily than the inner portions that are shielded by the outer regions. This tends to produce large nonuniformities in the liquid fraction across the layer. Consequently, to maintain a uniform liquid fraction, the required nonuniformity in velocity across the layer must be increased as the optical thickness increases; this is evident in Fig. 4. As the scattering albedo becomes larger, the increased energy reflection between the drops tends to equalize the energy being lost from each local dx region within the layer. Hence as Ω is increased, there is a decrease in the size of the velocity nonuniformity required to maintain the liquid fraction constant across the radiating layer. The combined effects of varying optical thickness and scattering albedo result in the trends in Fig. 4.

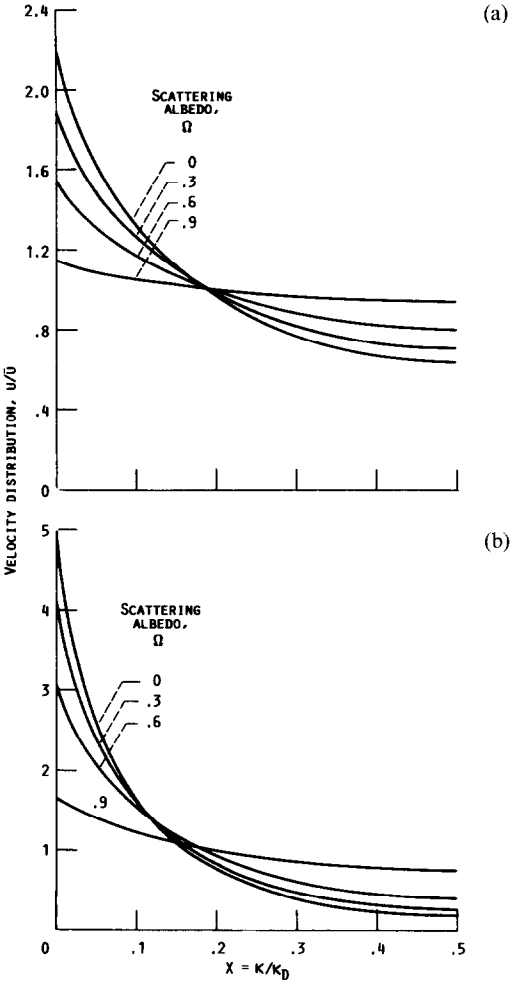

FIG. 4. Velocity distributions as a function of κ_D and Ω that will maintain a uniform liquid fraction across the layer: (a) optical thickness, $\kappa_D = 2$; (b) optical thickness, $\kappa_D = 5$.

REFERENCES

1. A. T. Mattick and A. Hertzberg, Liquid droplet radiators for heat rejection in space, *J. Energy* **5**, 387–393 (1981).
2. A. F. Presler, C. E. Coles, P. S. Diem-Kirsop and K. A. White, Liquid droplet radiator program at the NASA Lewis Research Center, ASME Paper 86-HT-15 (June 1986).
3. R. T. Taussig and A. T. Mattick, Droplet radiator systems for spacecraft thermal control, *J. Spacecraft Rockets* **23**, 10–17 (1986).
4. R. Siegel, Transient radiative cooling of a droplet-filled layer, *J. Heat Transfer* **109**, 159–164 (1987).
5. R. Siegel and J. R. Howell, *Thermal Radiation Heat Transfer*, 2nd Edn, Chap. 14. Hemisphere, Washington, DC (1981).